JOURNAL OF APPLIED ELECTROCHEMISTRY 27 (1997) 43–49

Electrode impedance parameters and internal resistance of a sealed $LiC/Li_{1-x}CoO_2$ lithium-ion rechargeable battery

V. GANESH KUMAR*, N. MUNICHANDRAIAH‡, A. K. SHUKLA*

Solid State and Structural Chemistry Unit and Department of Inorganic and Physical Chemistry‡, Indian Institute of Science, Bangalore-560 012, India*

Received 16 January 1996; revised 17 April 1996

The individual electrode impedance parameters and internal resistance of a sealed $LiC/Li_{1-x}CoO_2$ lithium-ion rechargeable battery were estimated by a galvanostatic nondestructive technique. Various resistive components of the battery were found to be minimum between state-of-charge values 0.5–0.9. It is expected that the operation of the battery within about 50% of its depth-of-discharge would prolong the charge/discharge cycle life of the battery.

1. Introduction

Effort is being made to develop ecofriendly, compact, light-weight and efficient rechargeable batteries to replace the ubiquitous Ni–Cd battery by the turn of this century in various consumer applications. To this end, rocking-chair lithium or lithium-ion rechargeable cells are envisaged as one of a favoured option [1].

A lithium-ion rechargeable cell consists of $LiCoO_2$-type cathode and a carbon anode. The open-circuit voltage of $LiC/Li_{1-x}CoO_2$ cell is 3.8 V at $x \approx 0$ which gradually increases to about 4.7 V with increasing x [2]. When charged to 4 V, the cathode has the chemical composition $Li_{0.5}CoO_2$ and remains isostructural with $LiCoO_2$ which has a layered structure analogous to $LiTiS_2$ except that the anions in the former adopt cubic close packing instead of hexagonal close packing. Lithium ions can be reversibly extracted from between the layers topotactically with concomitant oxidation of Co^{3+} to Co^{4+}.

The lithium-ion rechargeable cells, now commercially available from Sony Energytech Inc. in Japan, employ the following configuration [3, 4]:

$$LiC \,|\, PC + DME + LiPF_6(1\,M) \,|\, Li_{1-x}CoO_2$$

The nominal voltage of the Sony lithium-ion rechargeable battery with two cells of 3.6 V connected in series is 7.2 V. The energy density of the battery up to a cut-off voltage of 6 V is found to be about 100 Wh kg^{-1}.

The commercialization of lithium-ion battery by Sony is considered an important breakthrough in battery technology. However, the information on the performance features of the Sony lithium-ion rechargeable battery is lacking in the literature. A basic characterization of battery performance requires a knowledge of internal parameters such as charge-transfer resistance and double-layer capacitance of positive and negative electrodes individually, as well as the internal resistance. Evaluation of these parameters in a nondestructive way is a difficult task in a sealed battery. In a recent study [5] by using a.c. impedance technique, only the sums of charge-transfer resistances and double-layer capacitances of positive and negative electrodes of a sealed Pb-acid battery were evaluated.

In this study a galvanostatic non-destructive technique (GNDT), developed primarily by Sathyanarayana *et al.* [6] has been employed to evaluate the impedance parameters of the individual electrodes and internal resistance of the sealed $LiC/Li_{1-x}CoO_2$ lithium-ion battery at various states-of-charge (*SOC*), that is the ratio of available capacity to maximum attainable capacity. These data are central for optimum performance of $LiC/Li_{1-x}CoO_2$ lithium-ion rechargeable batteries.

2. Experimental details

Sony-NP510 lithium-ion rechargeable batteries with 1.25 Ah rated capacity (manufacturer's rating) and nominal voltage of 7.2 V were conditioned by conducting charge/discharge cycles at $C/10$ rate. The fully-conditioned batteries were found to yield a capacity of 1.125 Ah with the faradaic efficiency of about 97%. The charge and discharge cycles for the test batteries were restricted to cut-off-voltages of 8.4 and 6.0 V, respectively.

The electrical circuit employed for GNDT is essentially similar to that described in [6]. In brief, it consists of the test battery, a decade resistance box, a regulated d.c. power supply and a microswitch as shown schematically in Fig. 1. The GNDT involves discharge of the test battery at substantially low rate ($\sim C/100$) necessitating precise measurement of concomitant changes in its voltage. The voltage of the test battery was therefore required to be compensated by a GR-1455 A type voltage divider backed-up with a couple of conditioned 6 V/4 Ah Pb-acid batteries connected in series. This facilitated the measurement

0021-891X

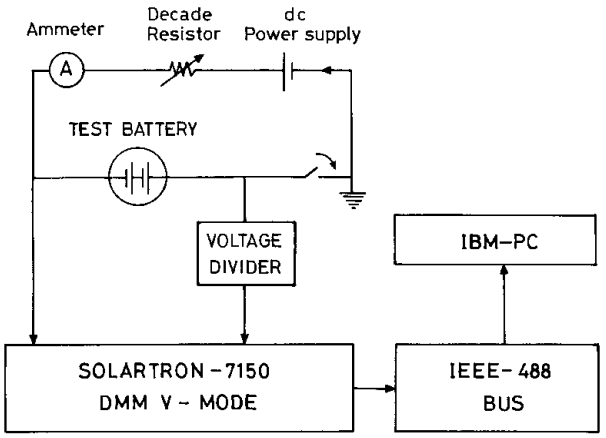

Fig. 1. Schematic set-up for digital recording of V–t transients under GNDT conditions.

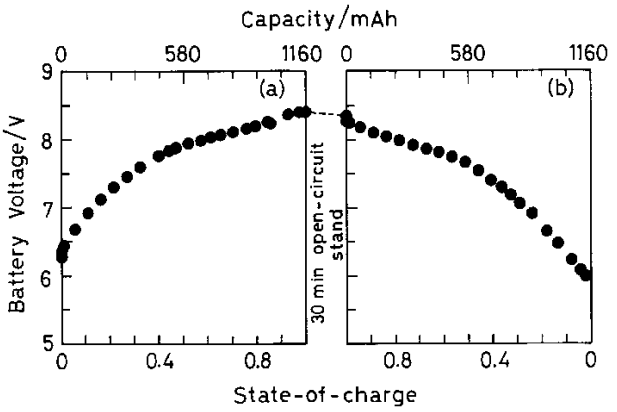

Fig. 2. Typical (a) charge and (b) discharge curves for the lithium-ion rechargeable test battery (charge current = discharge current = 125 mA $\approx C/10$ rate).

of compensated voltage (V) of the test battery at any instance with respect to its rest value (V^r), i.e. ($V - V^r$), using a high input-impedance Solartron-7150 digital multimeter interfaced to an IBM-PC through an IEEE-488 BUS. The data acquisition was driven with the aid of a program written in GW-BASIC. The data were collected for every 0.25 s over a duration of 150 s. All the experiments were done at 24 ± 1 °C. The noise level in data collected was below $\pm 20\,\mu$V. The data were further smoothed with the aid of the Mathematica Software. The data collection and analysis were carried out repeatedly at several states-of-charge of the test battery to ensure reproducibility. The impedance parameters were found to be within ±5% error.

3. Results and discussion

In a $LiC/Li_{1-x}CoO_2$ lithium-ion rechargeable cell, Li^+-ions are rocked back and forth between two intercalation electrodes during its charge and discharge processes. The anode and cathode of the cell intercalate/deintercalate during the charge/discharge processes as represented below:

$$LiCoO_2 + Li_{1-x}C \underset{\text{discharge}}{\overset{\text{charge}}{\rightleftharpoons}} Li_{1-x}CoO_2 + LiC \quad (1)$$

The charge/discharge data of the test battery at $C/10$ rate are shown in Fig. 2. The voltage during both the charge and discharge processes varies continuously with the state-of-charge of the battery. Such a behaviour in the variation of the battery voltage is expected for a battery employing intercalation materials as anode and/or cathode [7].

The equivalent circuit of the test battery under the conditions described in the experimental section is shown in Fig. 3, where T_1 and T_2 refer to the battery terminals, R_Ω is the ohmic resistance, $R_{t,1}$ and $C_{d,1}$ are charge-transfer resistance and interfacial capacitance (which includes double-layer capacitance and associated capacitive components due to adsorption, passive films etc.) for one of the electrodes; $R_{t,2}$ and $C_{d,2}$ are charge-transfer resistance and interfacial capacitance for the other electrode. As the discharge current (11.25 mA) corresponding to $C/100$ rate is sufficiently low and the measurements are restricted to a duration of a few minutes only, the SOC of the test battery could be taken to be nearly invariant; the variance in SOC being only 0.0004. Accordingly, it may be assumed that the electron-transfer processes are the rate-determining steps for both electrode reactions. Since the electrode processes are not governed by mass transfer, the Warburg components are not included in the equivalent circuit.

For a small current-perturbation, the voltage response of the test battery can be written with reference to the equivalent circuit shown in Fig. 3 as,

$$V^r - V = IR_\Omega + IR_{t,1}[1 - \exp(-t/\tau_1)] + IR_{t,2}[1 - \exp(-t/\tau_2)] \quad (2)$$

where I is the discharge current, τ_1 ($=R_{t,1}C_{d,1}$) and τ_2($=R_{t,2}C_{d,2}$) are the time constants of the electrode processes. The exponential terms in Equation 2 are due to the charging of $C_{d,1}$ and $C_{d,2}$. At times $t \geqslant \tau_1$ and τ_2, the capacitors attain complete charge and therefore the voltage drop is only due to resistive components, viz. $R_{t,1}$, $R_{t,2}$ and R_Ω.

A solution of Equation 2 with experimental data can provide the impedance parameters of the test battery. Since there are serious limitations in the direct algebraic procedure to solve Equation 2, an alternative approach described below in steps 1, 2 and 3 becomes imperative [8]. In this procedure, it is mandatory that the time constants τ_1 and τ_2 should be separable. This analysis is not satisfactory for a battery (or a cell) when $\tau_1 \approx \tau_2$. When $\tau_1 \ll \tau_2$ the

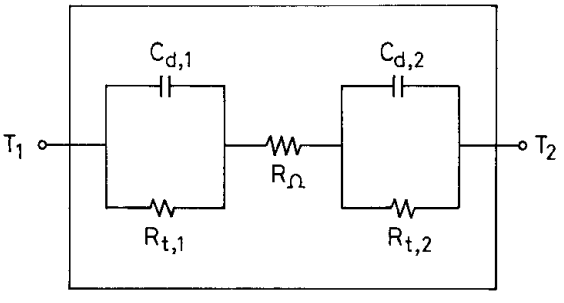

Fig. 3. Equivalent circuit for the test battery under the GNDT conditions.

analysis requires long-time data collection which may lead to a substantial change in SOC of the battery.

Step 1: Equation 2 shows that V against t is non-linear. Two instances at time t^* and t^{**}in the initial region of V/t curve are considered such that there is a measurable difference in the corresponding slopes (m^* and m^{**}) of the curve at these times. Although the time zone of these slopes is governed by the relaxation processes at both the electrodes, it is assigned entirely due to one of the processes, say τ_1-process. An approximate value of τ_1, namely τ_1' is given by

$$\tau_1' = \frac{t^{**} - t^*}{\ln(-m^*) - \ln(-m^{**})} \tag{3}$$

which is obtained by differentiating Equation 2 with respect to time (t) on neglecting the contribution from the τ_2-process.

Step 2: Since the function $(1 - \exp(-t/\tau))$ attains about 99% of its final value at $t = 5\tau$, it is assumed that the relaxation at $t \geq 5\tau_1'$ is only due to the τ_2-process.

Under this condition, Equation 2 reduces to

$$V^r - V = I(R_\Omega + R_{t,1}) + IR_{t,2}[1 - \exp(-t/\tau_2)] \tag{4}$$

which further yields,

$$\ln(-\mathrm{d}V/\mathrm{d}t) = \ln(IR_{t,2}/\tau_2) - t/\tau_2 \tag{5}$$

A linear plot of $\ln(-\mathrm{d}V/\mathrm{d}t)$ against t in the time domain $t > 5\tau_1'$ provides τ_2 and $R_{t,2}$ from its slope and intercept and hence $C_{d,2}$. Substitution of τ_2 in Equation 4 followed by a plot of $(V^r - V)$ against $\exp(-t/\tau_2)$ gives a straight line in the time domain $t > 5\tau_1'$. The intercept at $t = 0$ of the plot gives the value of the total internal resistance, $R_i (= R_\Omega + R_{t,1} + R_{t,2})$.

Step 3: Equation 2 is now recast as

$$Y = -IR_{t,1}\exp(-t/\tau_1) \tag{6}$$

where $Y = V^r - V - IR_i + IR_{t,2}\exp(-t/\tau_2)$

Therefore,

$$\ln(-Y) = \ln(IR_{t,1}) - t/\tau_1 \tag{7}$$

Since Y is now known completely at each t, a plot of $\ln(-Y)$ against t in the time domain $t < 5\tau_1'$ gives a straight line of slope $(-1/\tau_1)$ and intercept $IR_{t,1}$. This step provides the values of τ_1, $R_{t,1}$ and hence $C_{d,1}$. Thus, R_Ω can be calculated. All the five parameters, viz. R_Ω, $R_{t,1}$, $R_{t,2}$, $C_{d,1}$ and $C_{d,2}$ of the test battery are thus obtained nondestructively by a low-rate galvanostatic discharge of the battery for a short time. A critical examination of the above procedure by simulating voltage transients was carried out by Ilangovan and Sathyanarayana [6].

A typical galvanostatic discharge transient of the test battery at $SOC = 0.1$ for 230 s is shown in Fig. 4. The linear polarization domain of the GNDT is ensured by recording transients with several discharge currents close to $C/100$ and plotting $(V^r - V)/I$ against t. All the plots lie within an error of $\pm 3\%$ in a time zone up to 150 s, and hence the data within this duration are included in the analysis.

Employing Equation 3, τ_1' was calculated to be 14 s from the slopes of the voltage transient curve lying between 5–10 s. In the region $t > 5\tau'$ (~70 s), the plot of $\ln(-\mathrm{d}V/\mathrm{d}t)$ against t is a straight line between 70–140 s as shown in Fig. 5. From the slope and intercept of this plot, τ_2 and $R_{t,2}$ are calculated to be 123 s and 560 mΩ, respectively. Accordingly, the interfacial capacitance $C_{d,2}$ is estimated to be 220 F

By substituting the values of τ_2 in Equation 4, $(V^r - V)$ was plotted against $\exp(-t/\tau_2)$ in the time domain $t > 5\tau_1'$ as shown in Fig. 6. The total resistance

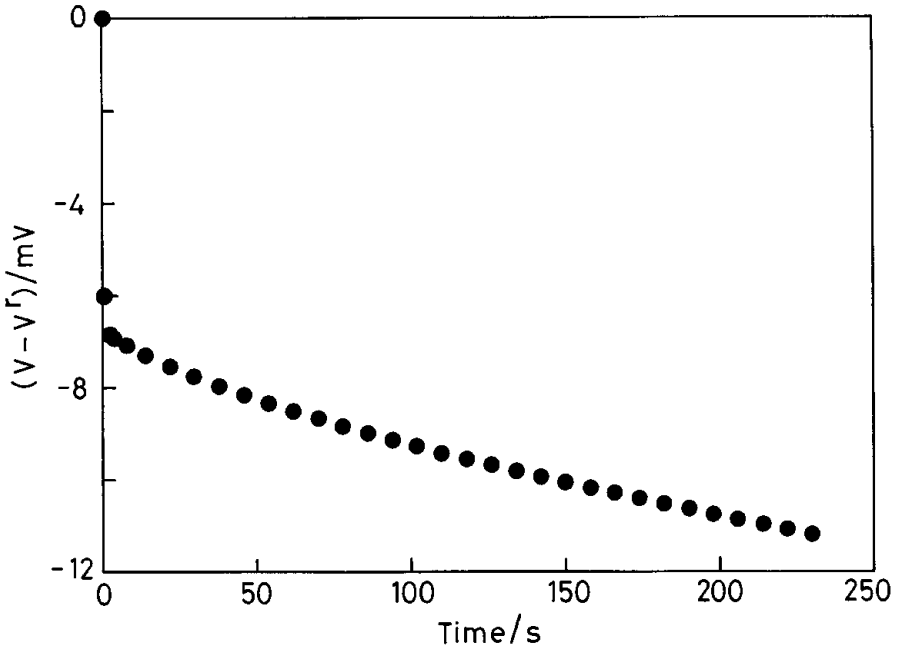

Fig. 4. Typical galvanostatic discharge transient (discharge current: 11.2 mA) of the test battery at $SOC = 0.1$. For the sake of brevity only 3% of the acquired data are shown.

$R_i(= R_\Omega + R_{t,1} + R_{t,2})$ is calculated from the intercept of the plot and is found to be 1.2Ω.

From the values of R_i, $R_{t,2}$ and τ_2, the values of Y were computed in the time domain $t < 5\tau_1'$, and ln $(-Y)$ plotted against t as shown in Fig. 7. From the slope and intercept, the values of τ_1 and $R_{t,1}$ were estimated to be 13 s and 18 mΩ, respectively. The interfacial capacitance $C_{d,1}$ is thus found to be 730 F. Thus the internal resistance R_Ω is 630 mΩ.

The resistive and reactive components of the lithium-ion rechargeable battery have been evaluated at different states-of-charge. The data are presented in Figs 8 and 9. It is interesting to note that both $R_{t,1}$ and $R_{t,2}$ show a minimum, with $C_{d,1}$ and $C_{d,2}$ exhibiting a maximum around $SOC = 0.7$. The electrochemical reactions at the two electrodes during charge/discharge processes of the test battery are

$$\mathrm{LiC} \underset{\text{charge}}{\overset{\text{discharge}}{\rightleftharpoons}} \mathrm{Li}_{1-x}\mathrm{C} + x\mathrm{Li}^+ + x\mathrm{e}^- \qquad (8)$$

$$\mathrm{Li}_{1-x}\mathrm{CoO}_2 + x\mathrm{Li}^+ + x\mathrm{e}^- \underset{\text{charge}}{\overset{\text{discharge}}{\rightleftharpoons}} \mathrm{LiCoO}_2 \qquad (9)$$

Prior to discussion on impedance parameters of the individual electrodes, it is essential to assign the observed features of electrodes 1 and 2 appropriately to the positive or negative electrodes of the test battery. The $R_{t,1}$ value lies between 5–40 mΩ (Fig. 8(a)) while $R_{t,2}$ ranges between 300–600 mΩ (Fig. 8(b)). It is reported that the impedance of the negative electrode of lithium-ion rechargeable cell similar to the test battery is about 60 mΩ [9]. Accordingly, electrodes 1 and 2 are the negative and positive electrodes of the test battery, respectively.

It is believed that the formation of a passive layer occurs on intercalated carbon electrodes similar to the lithium metal [9]. The passive film is electronically insulating but ionically conducting. At SOC values close to 1, the passive layer is likely to be thicker

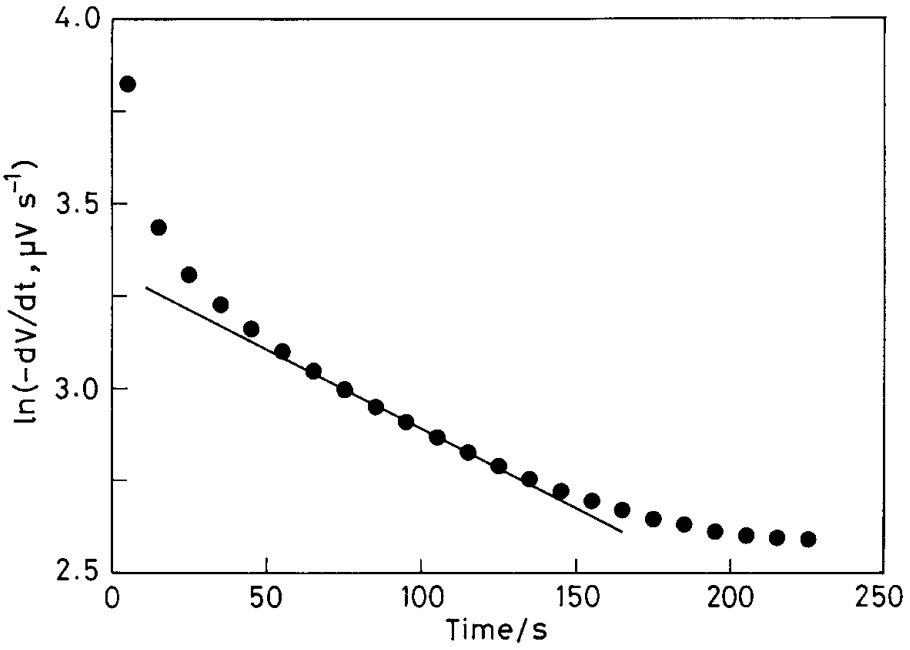

Fig. 5. Plot of ln $(-\mathrm{d}V/\mathrm{d}t)$ against time at $SOC = 0.1$ of the test battery.

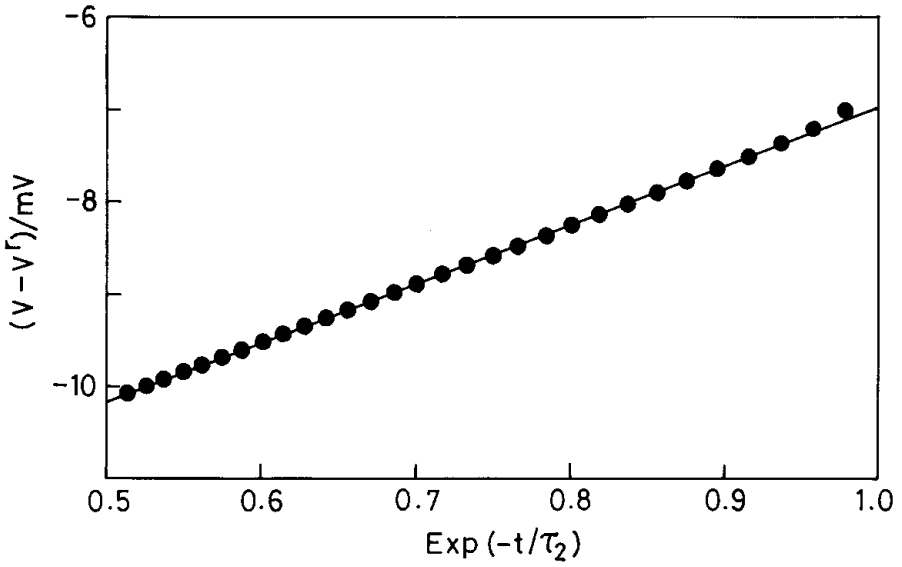

Fig. 6. Plot of $(V - V^r)$ against $\exp(-t/\tau_2)$ at $SOC = 0.1$ of the test battery.

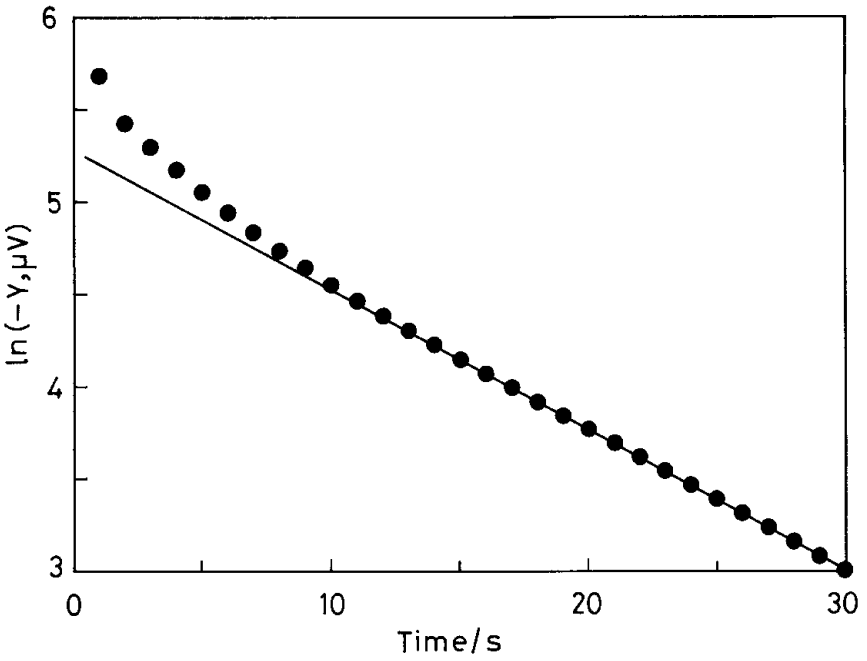

Fig. 7. Plot of $\ln(-Y)$ against time at $SOC = 0.1$ of the test battery.

and more resistive in relation to its value at lower SOC values. The charge-transfer resistance $R_{t,1}$ is therefore higher at $SOC \approx 1$ in relation to its value at $SOC \simeq 0.7$ (Fig. 8(a)).

As the battery discharge proceeds from its fully-charged state ($SOC = 1$), the activity of lithium in the carbon negative electrode depletes due to continuous lithium-deintercalation. In the linear polarization regime (i.e., at sufficiently small overpotential ($\eta \ll 26\,\text{mV}$)) the exchange current, I_o, can be expressed as $I_o = RT/nFR_{ct}$, where R_{ct} is the charge-transfer resistance ($= R_{t,1}$ in the present case). The exchange current density, i_o, is expressed as $i_o = I_o/A = nFk^\circ C$, where A is the geometrical area of the electrode, k^o is the standard rate constant, C is the concentration (activity) of the electroactive species, and n and F have their usual meanings. Since exchange current is proportional to the activity of the reactant ions, the observed increase in $R_{t,1}$ from $SOC \simeq 0.7$ down to $SOC \simeq 0$ could be attributed to depletion of lithium from carbon matrix. The combined effect of the passive layer and the activity of lithium reflects a minimum $R_{t,1}$ at SOC values between 0.5 and 0.7 as shown in Fig. 8(a). This suggests that the charge-

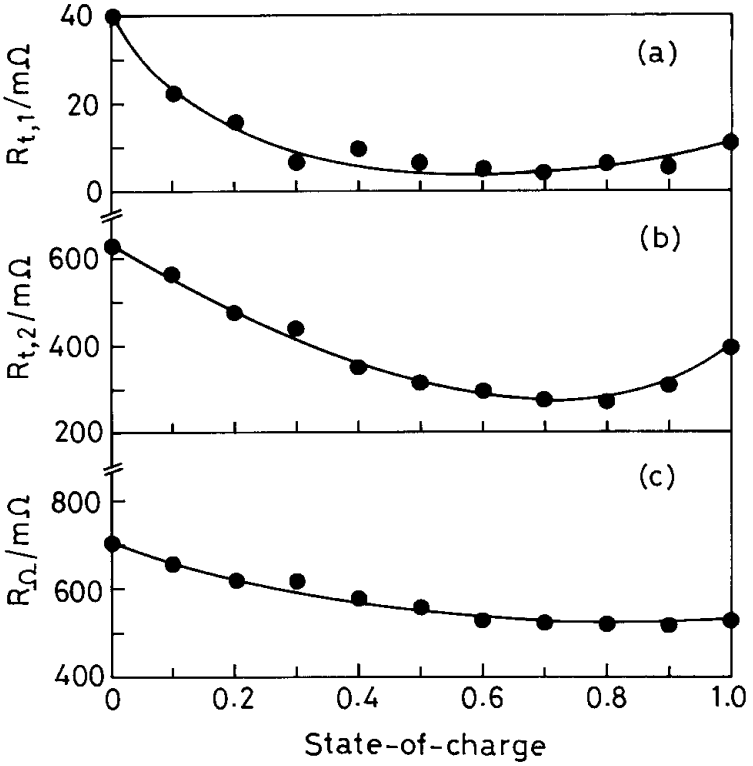

Fig. 8. Plot of resistive components of the test battery as function of itsSOC values.

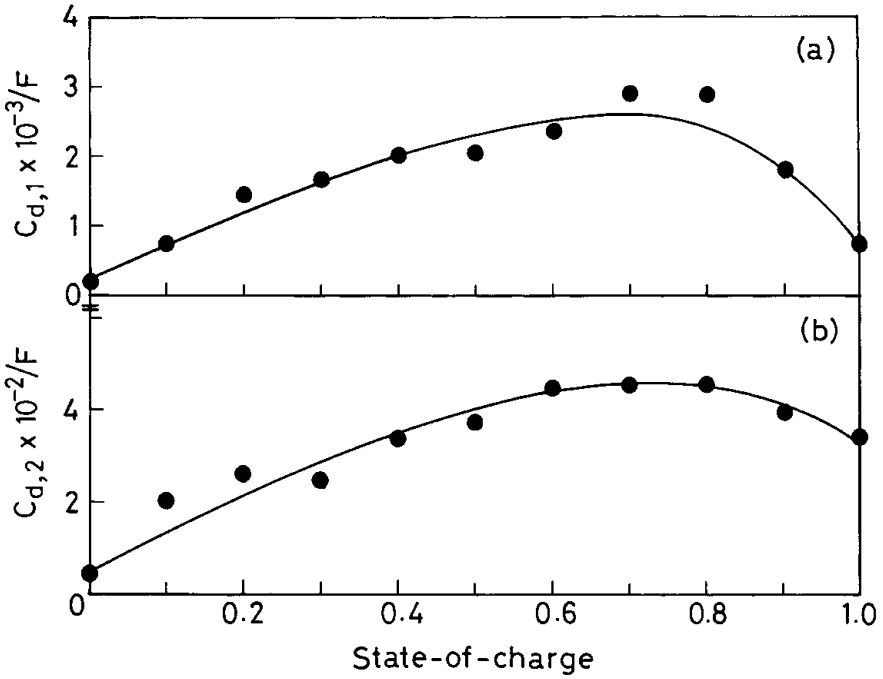

Fig. 9. Plot of capacitive components of the test battery as function of its*SOC* values.

transfer process at the negative electrode will proceed at a faster rate in a carbon electrode partially intercalated with lithium.

The capacitance $C_{d,1}$ is maximum in the *SOC* range between 0.6 to 0.9 as shown in Fig. 9(a), since there is a passive-film formation at the electrode at $SOC = 1$, its surface area is likely to be lesser in relation to other *SOC* values. Accordingly, $C_{d,1}$ will decrease at *SOC* values close to 1. By contrast, at *SOC* values less than 0.5, lithium activity in the negative electrode is low and corresponding electrochemical active area of the double layer is also small. As a result, $C_{d,1}$ decreases with the *SOC* value of the test battery. Interestingly, similar to $R_{t,1}$ and $C_{d,1}$, $R_{t,2}$ and $C_{d,2}$ (Fig. 9(b)) also show a minimum and a maximum in their values at *SOC* values between 0.5 and 0.9. The charge-transfer resistance $R_{t,2}$ is about 15 times higher than $R_{t,1}$. This suggests that Reaction 9 is less catalysed in relation to Reaction 8, assuming that the electrochemical active areas of both the electrodes are similar.

The magnitudes of the capacitive components, namely $C_{d,1}$ and $C_{d,2}$, are larger than the usual values reported for electrode/electrolyte interfaces; this is quite likely due to the high surface area ($10\,m^2\,g^{-1}$) of the electrode materials. Taking these surface area values, the interfacial capacitances for the electrodes are estimated to be $\sim 1\,mF\,cm^{-2}$ which are close to the reported values for battery electrodes [10–13]. It is noteworthy that capacitance values as high as 120 F have been reported [14] for the sintered nickel positive electrodes similar to the present results.

The combined ohmic resistances of the electrodes and the electrolyte in the test battery is reflected by R_Ω. The variation of R_Ω with the *SOC* of the test battery is shown in Fig. 8(c). there is a gradual decrease in R_Ω from $SOC = 0$ up to $SOC = 0.6$ and it is nearly invariant between *SOC* values 0.6 and 1. Since the electrolyte does not participate in the overall cell reaction, its composition and hence its conductivity should be invariant at all *SOC* values of the test battery. The anode of the test battery (electrode 1) is metallic and its electrical conductivity is not expected to change with SOC. By contrast, the cathode of the test battery (electrode 2) comprising $Li_{1-x}CoO_2$ is a semiconductor when $x = 0$, but its electrical conductivity gradually increases with increasing x in the composition [15]. This is reflected through a decrease in R_Ω between $SOC = 0$ and 0.6 beyond which it seems to have little effect.

4. Conclusion

The impedance parameters of the $LiC/Li_{1-x}CoO_2$ lithium-ion rechargeable battery deduced from this study reveal that the optimum performance of the battery is achieved at *SOC* values between 0.5–0.9. A reduction in the charge-transfer resistance at the positive electrodes of the battery is desirable to further its performance; improvements in the conductivity of the cathode material will also elevate the battery features. For the long cycle-life of the battery, it is recommended that the depth-of-discharge of the battery be restricted to about 50%.

Acknowledgements

We thank Dr S. Higuchi of Osaka National Research Institute, Japan for the supply of test batteries. Our thanks are also due to Dr S. Ilangovan, VSSC, Trivandrum for helpful discussions. Financial support from ISRO-IISc Space Technology Cell is gratefully acknowledged.

References

[1] D. Guyomard and J. M. Tarascon, *Adv. Mater.* **6** (1994) 408.
[2] K. Mizushima, P. C. Jones and J. B. Goodenough, *Mater. Res. Bull.* **15** (1980) 783.
[3] S. Hossain, *in* 'Handbook of Batteries' (edited by David Linden), McGraw-Hill, New York (1995) pp. 36.1–36.77.
[4] M. S. Whittingham, *in* Proceedings of the International Workshop on Advanced Batteries (Lithium Batteries), STA Japan (1995) pp. 12–21.
[5] P. R. Roberge, E. Halliop, G. Verville and J. Smit, *J. Power Sources* **32** (1990) 261.
[6] S. A. Ilangovan and S. Sathyanarayana, *J. Appl. Electrochem.* **22** (1992) 456.
[7] M. S. Whittingham, *in* 'Solid State Ionic Devices' (edited by B. V. R. Chowdari and S. Radhakrishna), World Scientific, Singapore (1988) pp. 55–74.
[8] S. A. Ilangovan, PhD thesis, Indian Institute of Science, Bangalore (1991).
[9] S. Megahed and B. Scrosati, *J. Power Sources* **51** (1994) 79.
[10] K. Vijayamohanan, A. K. Shukla, and S. Sathyanarayana, *J. Electroanal. Chem.* **295** (1990) 59.
[11] V. V. Batrakov and Z. A. Iofa, *Elektrokhimiya* **1** (1965) 123.
[12] S. Ya. Volosova, Z. A. Iofa and T. G. Stepina, *ibid.* **13** (1977) 393.
[13] S. P. Shavkunov, I. N. Sherstobitova and V. V. Kznetsov, *Elektrokhimiya* **19** (1983) 706.
[14] R. T. Barton, M. Huges, S. A. G. R. Karunathilaka and N. A. Hampson, *J. Appl. Electrochem.* **15** (1985) 399.
[15] G. Wei, T. E. Haas and R. B. Goldner, *Solid State Ionics* **58** (1992) 115.